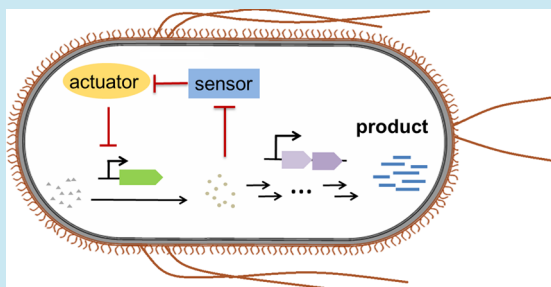


# Negative Feedback Regulation of Fatty Acid Production Based on a Malonyl-CoA Sensor–Actuator

Di Liu,<sup>†</sup> Yi Xiao,<sup>†</sup> Bradley S. Evans,<sup>‡</sup> and Fuzhong Zhang<sup>†,\*</sup><sup>†</sup>Department of Energy, Environmental and Chemical Engineering, Washington University, 1 Brookings Drive, St. Louis, Missouri 63130, United States<sup>‡</sup>Donald Danforth Plant Science Center, 975 North Warson Road, St. Louis, Missouri 63132, United States**S** Supporting Information

**ABSTRACT:** Engineering metabolic biosynthetic pathways has enabled the microbial production of many useful chemicals. However, pathway productivities and yields are often limited by metabolic imbalances. Synthetic regulatory circuits have been shown to be able to balance engineered pathways, improving titers and productivities. Here we developed a negative feedback regulatory circuit based on a malonyl-CoA-based sensor–actuator. Malonyl-CoA is biosynthesized from acetyl-CoA by the acetyl-CoA carboxylase, which is the rate-limiting step for fatty acid biosynthesis. Overexpression of acetyl-CoA carboxylase improves fatty acid production, but slows down cell growth. We have devised a malonyl-CoA sensor–actuator that controls gene expression levels based on intracellular malonyl-CoA concentrations. This sensor–actuator is used to construct a negative feedback circuit to regulate the expression of acetyl-CoA carboxylase. The negative feedback circuit is able to up-regulate acetyl-CoA carboxylase expression when the malonyl-CoA concentration is low and down-regulate acetyl-CoA carboxylase expression when excess amounts of malonyl-CoA have accumulated. We show that the regulatory circuit effectively alleviates the toxicity associated with acetyl-CoA carboxylase overexpression. When used to regulate the fatty acid pathway, the feedback circuit increases fatty acid titer and productivity by 34% and 33%, respectively.

**KEYWORDS:** metabolic control circuits, negative feedback, malonyl-CoA, dynamic regulation, synthetic biology



Engineered microbes have shown great potential as cell factories for the production of fuels,<sup>1,2</sup> chemicals,<sup>3</sup> pharmaceuticals,<sup>4,5</sup> nutraceuticals,<sup>6</sup> and materials,<sup>7</sup> etc. To make these technologies economically viable, it is important to obtain high yields and productivities. Common engineering strategies to improve yields and productivities include overexpressing bottleneck enzymes, bypassing native regulations, blocking competing pathways, genome-scale optimization,<sup>8–11</sup> etc. However, due to various reasons, such as imbalanced enzyme activities, engineered pathways often have imbalanced metabolism. Under these circumstances, enzymes or intermediates can accumulate to toxic levels, which inhibit cell growth and decrease production.<sup>8,12</sup>

An engineered metabolic pathway can potentially be balanced by manipulating the intracellular concentration of pathway enzymes. Enzyme concentrations can be controlled (1) at the DNA level by tuning gene copy numbers,<sup>13</sup> (2) at the transcription level by tuning the strength of promoters,<sup>14,15</sup> and (3) at the translation level by choosing a suitable ribosome binding site (RBS).<sup>16</sup> These strategies allow static control of enzymes levels, which are mostly constant during chemical production.

In contrast to the static controls, natural metabolic pathways are dynamically regulated according to cell metabolic status.<sup>17–19</sup> Some pathways are regulated by positive feedback

loops. As an example, seven out of eight genes in the *Saccharomyces cerevisiae* leucine biosynthesis pathway are positively regulated by the transcription factor Leu3, which is in turn activated by a pathway intermediate:  $\alpha$ -isopropyl-malate ( $\alpha$ IPM). As a result, leucine biosynthesis is positively controlled by the intermediate branching from the common precursor of branched-chain amino acid biosynthesis.<sup>20</sup> Similarly, negative feedback regulation that controls the concentration of certain metabolites is also found in nature.<sup>21</sup> For example, all the eight genes involved in *S. cerevisiae* arginine biosynthesis pathway are negatively regulated by the cellular level of arginine through a transcription factor ArgR.<sup>17</sup> These regulation systems allow cells to adjust metabolite concentrations at desirable levels, balancing the pathway for optimal cell growth.<sup>22</sup> The balanced pathway also prevents the biosynthesis of unnecessary RNAs, proteins, or metabolites, increasing the efficiency of energy and carbon usage.<sup>23</sup> On the basis of this concept, a synthetic regulatory system that detects key metabolic intermediates and regulates pathway gene expression according to intermediate

**Special Issue:** Circuits in Metabolic Engineering

**Received:** October 5, 2013

**Published:** December 30, 2013

Table 1. Plasmids Used in This Study

plasmids	replication origin	overexpressed operon	resistance	refs
pBFR1k-RFP	BBR1	P <sub>FRI</sub> - <i>rfp</i>	Kan <sup>R</sup>	this study
pA8c-FapR	p15A	P <sub>BAD</sub> - <i>fapR</i> ( <i>B. subtilis</i> )	Cm <sup>R</sup>	this study
pE7a-acc	ColE1	P <sub>T7</sub> - <i>acc</i> ( <i>E. coli</i> )	Amp <sup>R</sup>	this study
pE7a-yACC	ColE1	P <sub>T7</sub> - <i>acc</i> ( <i>S. cerevisiae</i> )	Amp <sup>R</sup>	this study
pBFR#k-RFP (#: 2–6)	BBR1	P <sub>FRI</sub> - <i>rfp</i>	Kan <sup>R</sup>	this study
pA8c-0	p15A	P <sub>BAD</sub> - <i>none</i>	Cm <sup>R</sup>	this study
pE7a-0	ColE1	P <sub>T7</sub> - <i>none</i>	Amp <sup>R</sup>	this study
pBFR1k-lacI-8FapR	BBR1	P <sub>FRI</sub> - <i>lacI</i> , P <sub>BAD</sub> - <i>fapR</i>	Kan <sup>R</sup>	this study
pBFR1k-lacI-8MFapR	BBR1	P <sub>FRI</sub> - <i>lacI</i> , P <sub>BAD</sub> - <i>mfapR</i>	Kan <sup>R</sup>	this study
pBFR1k-RFP-8FapR	BBR1	P <sub>FRI</sub> - <i>rfp</i> , P <sub>BAD</sub> - <i>fapR</i>	Kan <sup>R</sup>	this study
pBFR1k-RFP-8MFapR	BBR1	P <sub>FRI</sub> - <i>rfp</i> , P <sub>BAD</sub> - <i>mfapR</i>	Kan <sup>R</sup>	this study
pA2c-tesA	p15A	P <sub>tet</sub> - <i>tesA</i> ( <i>E. coli</i> )	Cm <sup>R</sup>	this study

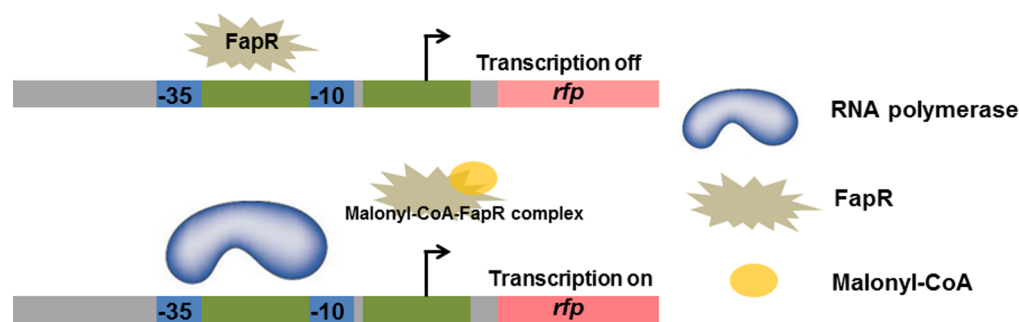


**Figure 1.** Malonyl-CoA sensor–actuator design. The FapR-binding sites are inserted flanking the  $-10$  region of the promoter (colored green). The presence of malonyl-CoA antagonizes the DNA binding activity of FapR and releases FapR from the engineered promoter, initiating RFP transcription.

concentrations could be used to balance its metabolism and improve product titers and yields.<sup>22,24</sup>

With the development of synthetic biology, several strategies now exist to create synthetic control circuits. One of the earliest metabolic regulatory circuits was constructed by harnessing an acetyl phosphate sensor to regulate lycopene biosynthesis.<sup>25</sup> In a recent study, a dynamic sensor–regulator system was built for an engineered pathway, in which expression levels of several heterologous genes were dynamically controlled by the concentration of a key metabolite, acyl-CoA.<sup>23</sup> In both systems the cells were able to dynamically modulate their metabolic flux in response to intracellular physiology and therefore dramatically improved production. Besides these experimental efforts, *in silico* simulations also predicted that dynamic pathway regulation could improve production.<sup>26–28</sup>

Here we report the development of a malonyl-CoA-based negative feedback system in *Escherichia coli* to improve fatty acid titer and productivity. Malonyl-CoA is a common building block for the biosynthesis of several types of compounds, including fatty acids, 3-hydroxypropionic acid, polyketides, and flavonoids.<sup>29,30</sup> These compounds can be used as or converted to biofuels, commodity chemicals, fine chemicals, and drugs. Bioproduction of fatty acids is particularly important because fatty acid derivatives provide renewable transportation fuels.<sup>31,32</sup> In *E. coli*, malonyl-CoA is biosynthesized from acetyl-CoA by acetyl-CoA carboxylase encoded by *accABCD* (*acc*). The *E. coli* acetyl-CoA carboxylase consists of four subunits: a biotin carboxyl carrier protein, a biotin carboxylase, and two carboxyltransferase subunits. This is the first step of fatty acid biosynthesis and is believed to be the rate-limiting step.<sup>33,34</sup> Several studies have shown that overexpression of *acc* genes improved both fatty acid and flavonoid production.<sup>35–38</sup>

On the other hand, overexpression of *acc* is toxic to cells.<sup>34,36</sup> The exact molecular mechanism of the toxicity is currently unclear. Possible reasons include the depletion of free CoA pool by malonyl-CoA overproduction, or the interference with biotin-utilizing enzymes by the imbalanced expression of the biotin carboxylase subunit.<sup>34</sup> To enhance malonyl-CoA supply while alleviating the toxicity caused by *acc* overexpression, we have devised a malonyl-CoA sensor–actuator and used it to negatively regulate *acc* expression. We have shown that the malonyl-CoA-based negative control system can alleviate the toxicity caused by *acc* overexpression. When the system was applied to fatty acid pathway, it improved both fatty acid titer and productivity by 34% and 33%, respectively.

## RESULTS AND DISCUSSION

We designed the malonyl-CoA sensor–actuator based on a naturally occurring malonyl-CoA-responsive transcription factor, FapR, from the Gram-positive bacteria *Bacillus subtilis*.<sup>39</sup> FapR specifically binds to a 17-bp DNA sequence and negatively regulates fatty acid and phospholipid metabolism in *B. subtilis*.<sup>40</sup> The binding of malonyl-CoA to FapR triggers a conformation change to the FapR, causing FapR–DNA complex to dissociate.<sup>39</sup> To our knowledge, such a malonyl-CoA-responsive transcription factor is absent in *E. coli*. To create malonyl-CoA biosensors in *E. coli*, we cloned the *B. subtilis* *fapR* gene into *E. coli* using a low copy number plasmid under the control of a P<sub>BAD</sub> promoter (pA8c-*fapR*, Table 1). Meanwhile, we constructed a FapR-regulated synthetic promoter (P<sub>FRI</sub>, the actuator) by inserting the 17-bp FapR-binding sequence into two regions flanking the  $-10$  region of a phage P<sub>A1</sub> promoter<sup>41</sup> (see Table 3). The actuator was later cloned to control the expression of a red fluorescence protein

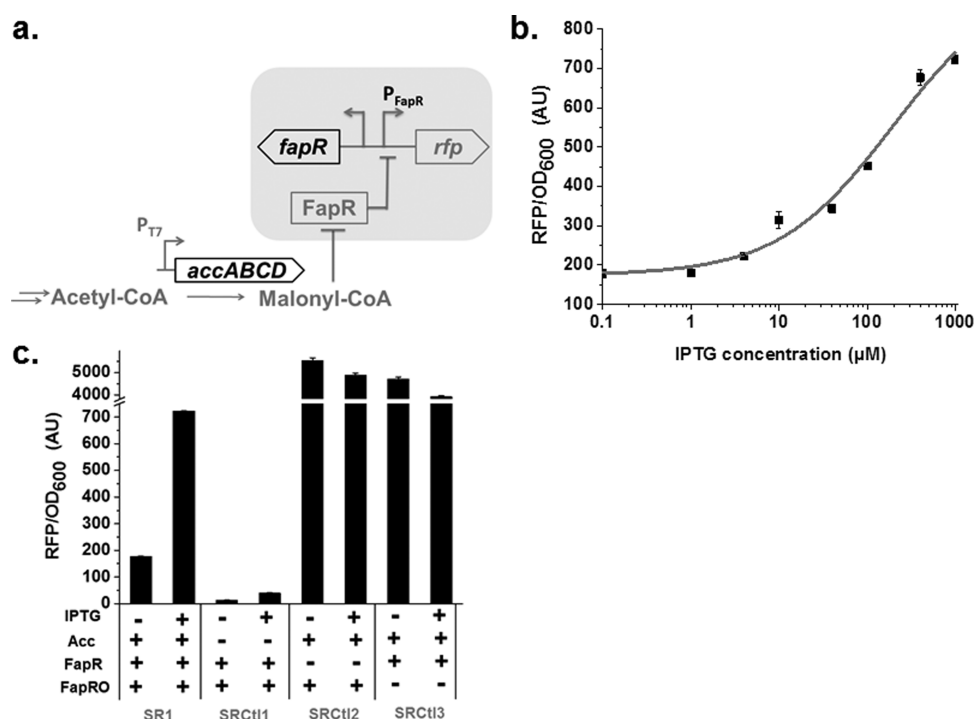


**Figure 2.** Characterization of malonyl-CoA sensor–actuator. (a) The malonyl-CoA sensor–actuator consists of a constantly expressed FapR, an engineered promoter–reporter system, and the *acc* under  $P_{T7}$ .  $P_{FapR}$  represents FapR-responsive promoter, e.g.  $P_{FR1}$ . (b) Response of malonyl-CoA sensor–actuator to IPTG. Strain SR1 was titrated with IPTG to vary cellular malonyl-CoA concentrations. Cell culture fluorescence was measured after 24 h and normalized by relative OD<sub>600</sub> using a fluorescence plate reader. (c) Response of control strains with individual Acc, FapR, and FapRO knockouts. Strains SRCtl1, SRCtl2, and SRCtl3 were cultivated with or without IPTG induction for malonyl-CoA accumulation. After 24 h, cell culture fluorescence was measured and normalized by relative OD<sub>600</sub>.

**Table 2. Strains Used in This Study**

strains	relevant genotype	refs
SAcc1	<i>E. coli</i> BL21 (DE3): pE7a-acc	this study
SAcc2	<i>E. coli</i> BL21 (DE3): pE7a-γACC	this study
SR1	<i>E. coli</i> BL21 (DE3): pBFR1k-RFP, pA8c-FapR, pE7a-acc	this study
SR2	<i>E. coli</i> BL21 (DE3): pBFR2k-RFP, pA8c-FapR, pE7a-acc	this study
SR3	<i>E. coli</i> BL21 (DE3): pBFR3k-RFP, pA8c-FapR, pE7a-acc	this study
SR4	<i>E. coli</i> BL21 (DE3): pBFR4k-RFP, pA8c-FapR, pE7a-acc	this study
SR5	<i>E. coli</i> BL21 (DE3): pBFR5k-RFP, pA8c-FapR, pE7a-acc	this study
SRCtl1	<i>E. coli</i> BL21 (DE3): pBFR1k-RFP, pA8c-FapR, pE7a-0	this study
SRCtl2	<i>E. coli</i> BL21 (DE3): pBFR1k-RFP, pA8c-0, pE7a-acc	this study
SRCtl3	<i>E. coli</i> BL21 (DE3): pBFR6k-RFP, pA8c-FapR, pE7a-acc	this study
FA1	<i>E. coli</i> BL21 (DE3): pA2c-tesA	this study
FA2	<i>E. coli</i> BL21 (DE3): pBFR1k-RFP-8FapR, pE7a-acc, pA2c-tesA	this study
FA3	<i>E. coli</i> BL21 (DE3): pBFR1k-lacI-8FapR, pE7a-acc, pA2c-tesA	this study
MFA2	<i>E. coli</i> BL21 (DE3): pBFR1k-RFP-8MFapR, pE7a-acc, pA2c-tesA	this study
MFA3	<i>E. coli</i> BL21 (DE3): pBFR1k-lacI-8MFapR, pE7a-acc, pA2c-tesA	this study

gene (*rfp*), resulting in plasmid pBFR1k-rfp. In the absence of malonyl-CoA, FapR is expected to bind to the 17-bp DNA sequence, which poses steric hindrance to RNA polymerase binding and inhibits RFP transcription. When malonyl-CoA is present, the binding of malonyl-CoA to FapR is expected to release FapR from the promoter ( $P_{FR1}$ ), enhancing RFP transcription (Figure 1).

To evaluate the malonyl-CoA sensor–actuator, we varied the intracellular malonyl-CoA concentrations using a malonyl-CoA-accumulating plasmid, pE7a-acc. Specifically, pE7a-acc contained an additional copy of the *E. coli acc* genes under the control of two T7 promoters so that the intracellular malonyl-CoA concentration could be varied by titrating the media with

IPTG (Figure 2a). We cotransformed pE7a-acc with the sensor–actuator plasmids, pA8c-FapR and pBFR1k-RFP, and cultivated the strain (SR1, Table 2) in LB medium. Cell culture fluorescence (normalized by cell density) at various IPTG concentrations was measured. As expected, cell culture fluorescence was increased by 4-fold with increasing IPTG concentrations (Figure 2b).

We next verified that the sensor–actuator worked according to the mechanism we designed by individually removing Acc, FapR, and the FapR operator site (FapRO) from the system, yielding three control strains (SRCtl1, SRCtl2, SRCtl3, Table 2). The cell culture fluorescence of these strains was measured with or without induction for malonyl-CoA accumulation

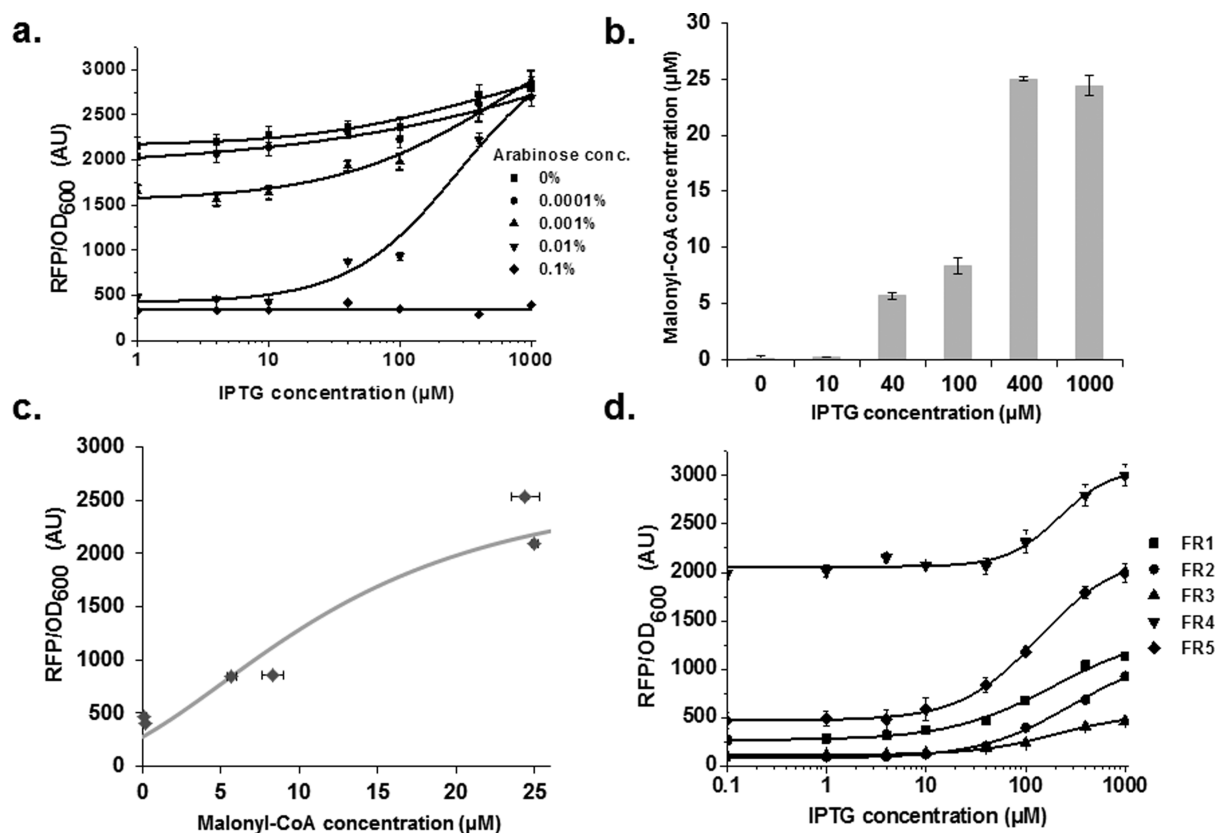


**Figure 3.** Characterization of malonyl-CoA sensor–actuator in minimal medium containing 2% glucose and its tuning to expand the output range. (a) Tuning of sensor–actuator in minimal medium by titrating arabinose (0% to 0.1%) to change the amount of FapR. IPTG was titrated to vary cellular malonyl-CoA concentration of strain SR1. Normalized cell culture fluorescence was measured 24 h after induction. (b) LC–MS quantification of malonyl-CoA concentrations of strain SAcc1 at various *acc* induction levels. (c) Response of the sensor–actuator to malonyl-CoA in minimal medium. The results were fitted to a thermodynamic model. The fitted  $K_d$  for malonyl-CoA–FapR binding was 6.3  $\mu\text{M}$ . (d) Tuning of malonyl-CoA sensor–actuator in LB medium. Promoters  $P_{FR2}$ – $P_{FR5}$  carried mutations at either the FapR binding site or the  $-10/-35$  region of  $P_{FR1}$  (Table 3). The corresponding sensor–actuator strains, SR2–SR5, were cultivated, and their normalized cell culture fluorescence at various IPTG concentrations was measured.

(Figure 2c). In the strain lacking the *Acc* plasmid (SRctl1, see Methods), cell culture fluorescence remained at basal levels, regardless of the inducer, indicating that malonyl-CoA synthesized from the genomic enzymes was not sufficient to turn on the sensor. In fact, fluorescence of strain SRctl1 (normalized fluorescence  $13.3 \pm 0.8$  au) was lower than that of strain SR1 under the noninducible condition (0 IPTG, normalized fluorescence  $177.8 \pm 0.3$  au), suggesting that in the latter case, there was leaky expression of *acc* from the T7 promoter, causing a slight increase in malonyl-CoA concentration. When either FapR or FapRO was removed, the promoter constantly remained at high expression levels, confirming our design that the promoter was repressed by FapR at the FapRO sites. As compared with these two nonrepressive strains (normalized fluorescence  $\sim 4500$  au), the SR1 strain exhibited a maximal fluorescence of  $743 \pm 0.5$  au (with 1 mM IPTG induction), indicating that the malonyl-CoA accumulated under this condition in LB medium was not sufficient to fully turn on the promoter. Overall, we have shown that the malonyl-CoA sensor–actuator responded specifically to cellular malonyl-CoA concentrations through FapR and FapRO.

Next we tested the behavior of the sensor–actuator in M9 medium containing 2% glucose, the medium usually used for chemical production. This would allow us to learn the behavior of the sensor–actuator for pathway regulation during

production. Due to catabolic repression of the  $P_{BAD}$  promoter in the glucose-rich M9 medium, less FapR was expressed compared to that in LB medium, leading to enhanced fluorescence (Figure 3a). To obtain optimal sensor–actuator behavior, we tuned the FapR expression level by titrating with various amounts of arabinose and examined the responses of the sensor–actuator strain. When a high arabinose concentration was used (0.1%), a large amount of FapR was expressed, leading to no malonyl-CoA activation even with 1 mM of IPTG induction (Figure 3a). By contrast, strains with low arabinose concentration produced an insufficient amount of FapR, resulting in an *rfp* expression that was not responsive to malonyl-CoA. The desired malonyl-CoA response was obtained with the addition of 0.01% arabinose, indicating that the amount of FapR produced under this condition was optimal for regulation. Although the current strain requires the addition of 0.01% arabinose to achieve an optimal FapR level in the M9/glucose medium, the need for inducer can be potentially eliminated by using a constitutive promoter with the proper strength to drive FapR expression.

To quantitatively evaluate the sensor–actuator, we used LC–MS to measure the accumulated malonyl-CoA concentrations under various induction levels in M9/glucose medium. With the plasmid pE7a-*acc*, cellular malonyl-CoA concentrations of strain SAcc1 (Table 2) increased from  $0.14 \pm 0.1$   $\mu\text{M}$  to  $24.4 \pm 0.9$   $\mu\text{M}$  when IPTG concentration was increased

**Table 3. Sequences of Engineered Malonyl-CoA-Responsive Promoters; Bold Sequences Represent the  $-35$  and  $-10$  Regions; FapR Binding Sites Are Underlined**

promoter	sequence
P <sub>FR1</sub>	AAAAAGAGTGTGACTT <u>TTAGTACCTGATACTAA</u> GATACTTAGATTCTTAGTACCTGATACTAAACC
P <sub>FR2</sub>	AAAAAGAGTGTGACTT <u>TTAGTACCTGATACTAA</u> GATACTT <u>TTAGTACCTGATACTAA</u> TACAGATACC
P <sub>FR3</sub>	AAAAAGAGTGTGACTT <u>TTAGTACTGATACTAA</u> GATACTTAGATTCA <u>TTTATGCTTCCGGCTCACC</u>
P <sub>FR4</sub>	AAAAAGAGTGTGACTT <u>TTAGTAACGGATACTAA</u> GATACTTAGGATTCTTAGTACCAGATACTAAACC
P <sub>FR5</sub>	GACGAATATATTGCCATGTGAAAAAATAGGATAGAATTAGTACCTGATACTAA <u>TAACAGATACC</u>
P <sub>FR6</sub>	AAAAAGAGTGTGACTT <u>TTAGTACTGATACTAA</u> GATACTTAGATTCA <u>TTTATGCTTCCGGCTCACC</u>

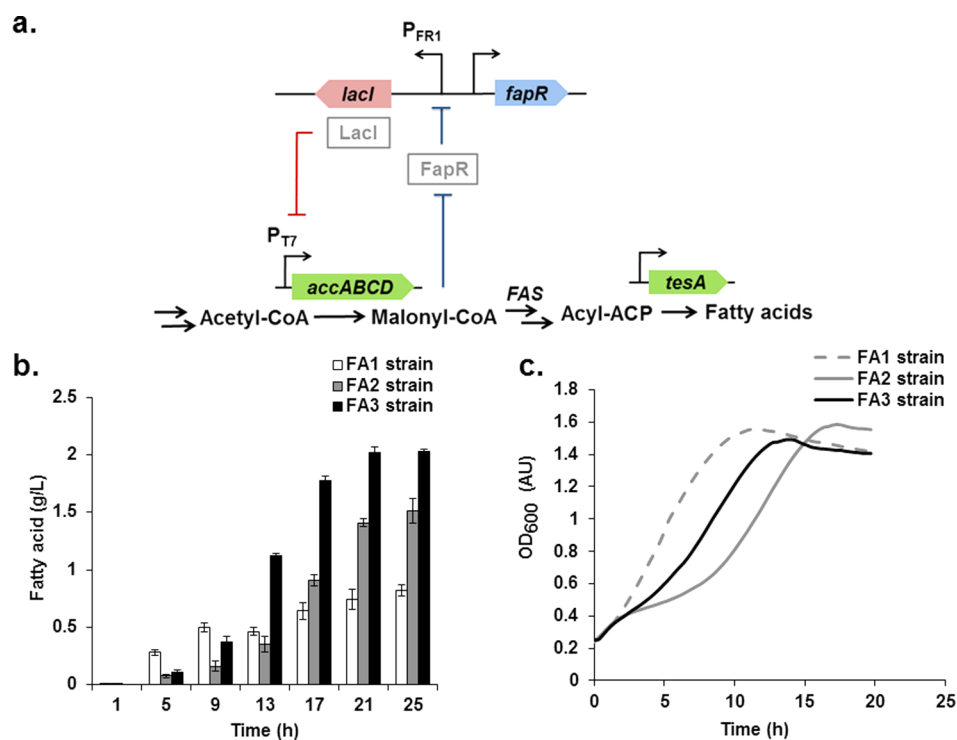


**Figure 4.** Construction of a negative feedback regulatory circuit and its effects on improving fatty acid titer and cell growth. (a) Negative feedback circuit design to regulate fatty acid production. A cytoplasmic thioesterase gene (encoded by *tesA*) was controlled by P<sub>Tet</sub> to produce fatty acids. The *acc* genes were controlled by a LacI-repressed P<sub>T7</sub> promoter. LacI expression was controlled by the P<sub>FR1</sub> that was repressed by FapR, which was further controlled by malonyl-CoA. When excess malonyl-CoA is accumulated, the biosensor will turn on the expression of *lacI*, which down-regulates *acc* expression, alleviating toxicity caused by *acc* overexpression. (b) Time course analysis of fatty acid titers from strain FA1 (white column), FA2 (gray column), and FA3 (black column). Strains were cultured in minimal medium with 2% glucose at 37 °C in shaking flasks. Fatty acid production titers were analyzed as described in Methods. (c) Cell growth of strains FA1 (dotted gray curve), FA2 (solid gray curve), and FA3 (black curve) were monitored in a plate reader until they reached the stationary phase.

from 0 to 1 mM (Figure 3b). This data allowed us to obtain a fluorescence/malonyl-CoA concentration curve, assuming strains SAcc1 and SR1 accumulated the same amount of malonyl-CoA under the same induction conditions (Figure 3c). Next, we fitted the data to a thermodynamic model modified from previous studies involved in inducible systems (Supporting Information [SI]).<sup>42</sup> Although we had only a few experimental data points due to the difficulties in accumulating malonyl-CoA to desirable levels and the challenges associated with malonyl-CoA quantification, our fitted binding constant for FapR–malonyl-CoA interaction, 6.3  $\mu$ M, was in the same order of magnitude as the value determined by *in vitro* isothermal titration calorimetry (2.4  $\mu$ M).<sup>39</sup>

We also sought to expand the capability of the malonyl-CoA sensor–actuator by tuning its output range. The behavior of the sensor–actuator is determined on the basis of the thermodynamic model, by the interaction between the promoter with FapR and the RNA polymerase. Both of these interactions can

be tuned by changing the promoter sequence. We modified the P<sub>FR1</sub> by introducing mutations to the FapR binding site and to the  $-35$  and  $-10$  regions of the promoter, leading to a series of P<sub>FR1</sub> variants (P<sub>FR2</sub>–P<sub>FR5</sub>, Table 3). We cloned the *rfp* 3' of each promoter and characterized them (strains SR2–SR5, Table 2) using cell culture fluorescence. These promoters positively responded to increasing *acc* induction levels and generated different RFP intensities, exhibiting varied strengths and dynamic ranges (Figure 3d). Overall, these promoters allow the expression levels of the malonyl-CoA-regulated genes to be tuned across a broad range.

In general, the fluorescence based malonyl-CoA sensor–actuator provides a comparative method for measuring intracellular malonyl-CoA concentrations. It avoids the labor-intensive extraction procedures using analytical quantification and the experimental errors caused by hydrolysis during sample preparation. Furthermore, the fluorescence-based measurement is quick and easy, allowing high-throughput analysis of a large

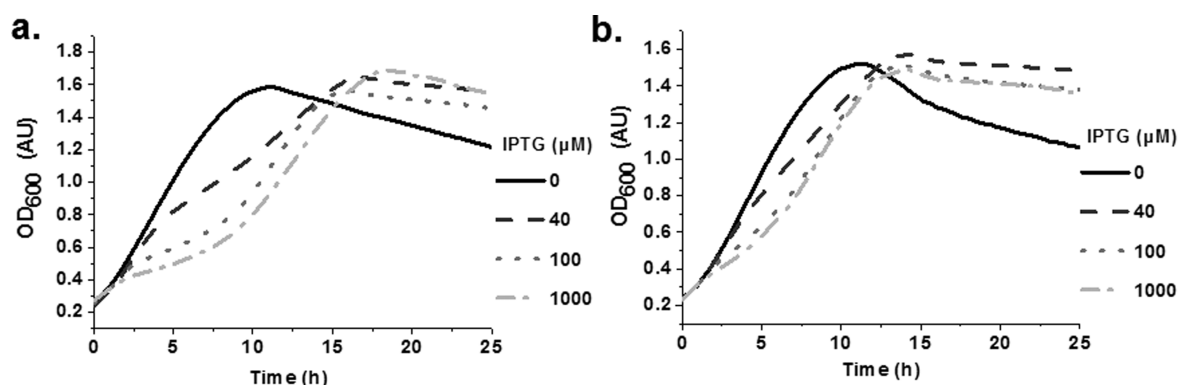


**Figure 5.** Effects of negative feedback regulatory circuit on cell growth. Cell growth was monitored for fatty acid-producing strains with (b, FA3 strain) and without (a, FA2 strain) the regulatory circuit under different *acc* induction levels. Cells were cultivated in minimal medium containing 2% glucose. Growth curves were monitored on a plate reader (see Methods). Note that the relative OD<sub>600</sub>'s are cell culture absorption (in arbitrary units) recorded from the plate reader under instrumental parameter settings as described in Methods.

number of samples. More importantly, the malonyl-CoA-based sensor–actuators can be used to regulate malonyl-CoA-involved metabolic pathways.

It has been previously shown in several studies that efforts to enhance the cellular malonyl-CoA pool by overexpressing acetyl-CoA carboxylase led to reduced cell growth due to toxicity.<sup>34,36</sup> To evaluate the toxicity, we overexpressed acetyl-CoA carboxylases from both *E. coli* and *S. cerevisiae* to different expression levels. Cell growth was measured, and the stationary phase cell densities (OD<sub>600</sub> at 20 h after IPTG induction) of different cultures were plotted against the different induction levels (Figure S1 in SI). Our data showed that overexpression of both acetyl-CoA carboxylase enzymes were toxic. We also evaluated the effects of *acc* overexpression on fatty acid production. Free fatty acids can be produced in *E. coli* by the overexpression of a cytosolic thioesterase (encoded by a leader sequence-deleted *tesA*), which hydrolyzes acyl-ACPs and releases free fatty acids. Previous expression of *tesA* in a *fadE* gene knockout strain led to the production of fatty acid at 1.2 g/L after three days cultivation in M9 medium containing 2% glucose.<sup>43</sup> To control the expression of *tesA* and *acc* separately, we placed the *tesA* under the control of an aTc-inducible promoter P<sub>Tet</sub>. As compared to the strain that only overexpressed the thioesterase (strain FA1), the strain with overexpression of *tesA* and *acc* (strain FA2) increased the fatty acid titer by 84% (Figure 4b), although it grew more slowly (Figure 4c). Both the increased free fatty acid titer and decreased cell growth are consistent with previous studies.<sup>29,34,44</sup>

Next we sought to develop a negative feedback circuit to tightly control the expression of acetyl-CoA carboxylase by sensing the cellular malonyl-CoA concentration. Ideally, we need the system to express *acc* when the malonyl-CoA concentration is low and to turn the *acc* expression down when the malonyl-CoA concentration is too high. Since the sensor–actuator positively responds to malonyl-CoA (a higher malonyl-CoA level leads to higher expression), an inverter was needed to complete a negative feedback circuit. To complete the circuit, we placed the *acc* under the control of a LacI-repressive T7 promoter, P<sub>T7</sub>, and placed the *lacI* under the control of P<sub>FRI</sub> (Figure 4a; Strain FA3, Table 2). With this design, IPTG induction initiates *acc* expression, which produces malonyl-CoA. When excess malonyl-CoA is accumulated in this strain (FA3), the malonyl-CoA sensor–actuator will turn on *lacI* expression, which in turn down-regulates *acc*, decreasing

the malonyl-CoA synthesis rate. The control strain (FA2) has the *lacI* replaced by the *rfp*, so that its *acc* is controlled by P<sub>T7</sub> and not the malonyl-CoA-regulated promoter.

We examined whether the negative feedback regulation circuit could alleviate the toxicity caused by *acc* overexpression. We monitored cell growth under fatty acid production conditions. FA2 and FA3 strains were cultured in minimal medium and induced for both fatty acid production and *acc* expression (using various amounts of IPTG). Cell growth was monitored continuously on the plate reader until the stationary phase was reached (Figure 5a and b). Compared to the FA2 strain, the FA3 strain had less growth inhibition, consistent with our design that the negative regulation circuit was able to control the *acc* expression level and to alleviate the toxicity, resulting in improved cell growth (Figure S2 in SI). Cell growth inhibition was observed at an IPTG concentration higher than 40 μM, which corresponded to  $5.7 \pm 0.3$  μM of malonyl-CoA. It is important to note that this malonyl-CoA concentration matches the fitted  $K_d$  (6.3 μM) of the sensor–regulator, which suggests that the designed sensor–actuator could respond to malonyl-CoA at a metabolically relevant concentration.

Last, we tested the effect of the negative feedback regulation circuit on fatty acid production. Fatty acid titers were measured at several time points during the exponential and early stationary phases (the first 25 h). As shown above, overexpression of *acc* from an inducible promoter increased fatty acid titer (strain FA2 compared to strain FA1). When the negative regulation circuit was used, the FA3 strain further increased the fatty acid titer (Figure 4b). After 25 h, the FA3 strain produced  $2.03 \pm 0.1$  g/L of fatty acids, being 34% higher than that of the FA2 strain. Furthermore, the FA3 strain had a fatty acid productivity of  $4.2 \pm 0.2$  g/(L·d), being 33% higher than that of the FA2 strain, which was  $3.2 \pm 0.1$  g/(L·d). Due to the alleviated toxicity effect, the negative-regulated strain entered the exponential growth phase earlier. This is particularly important for industrial applications, as minimizing fermentation time and maximizing productivity are pursued. Overall, our data indicate that the negative regulatory system can not only alleviate the toxicity that inhibits cell growth but also improve fatty acid titer and productivity.

To verify that the improved fatty acid titer was caused by the negative feedback circuit, we replaced the FapR of the FA2 and FA3 strains with a FapR double mutant (R106A and G107V), resulting in two additional control strains MFA2 and MFA3 (Table 2). Previous study has shown that the FapR double

mutant could bind to the FapRO site with the same affinity as that of the wild-type FapR, but could not interact with malonyl-CoA effectively.<sup>39</sup> Thus, the resulting control strain, MFA3, only differs from FA3 by two amino acids in FapR but does not have the feedback regulation due to the disrupted malonyl-CoA/FapR interaction. As a result, the reduced cell growth inhibition observed in FA3 strain was not observed in MFA3 strain (Figure S3 in SI). Furthermore, fatty acid titers of both MFA2 and MFA3 strains were similar to that of FA2 strain but less than that of the negative feedback-regulated FA3 strain (Figure S4 in SI). Overall, our results demonstrated that strains with a disrupted feedback circuit could neither reduce cell growth inhibition nor enhance fatty acid titer.

To further verify that the improved fatty acid titer is caused by the negative feedback regulation, rather than the use of different genetic constructs, we titrated the *acc* expression levels of the FA2 strain that used the inducible system with a broad range of IPTG concentrations (from 0 to 1 mM, Figure S4 in SI). Under all conditions, the maximal fatty acid titer produced by the inducible system was  $1.59 \pm 0.21$  g/L, being 22% lower than that of the negative regulation strain, FA3. In addition, further optimization of the negative feedback circuit, especially by tuning the concentration of the LacI repressor using the  $P_{FR1}$  variants ( $P_{FR2}$ – $P_{FR5}$ ), might further increase titers and productivities.

Overall, we have demonstrated that the negative feedback circuit has alleviated growth inhibition caused by either acetyl-CoA carboxylase overexpression or malonyl-CoA accumulation, improving fatty acid titers and productivities. This method can be readily extended to the production of other chemicals that use malonyl-CoA as a precursor, such as flavonoids and polyketides, to improve cell growth and enhance productivities. Similar sensor–actuators can be designed to sense other critical cell metabolites. At last, the negative feedback circuit design strategy can be implemented to other systems, alleviating the toxicity caused by protein overexpression or metabolite intermediate accumulation, to enhance the titer and productivity of various chemicals.

## METHODS

**Materials.** Phusion DNA polymerase was purchased from New England Biolabs (Beverly, MA, U.S.A.). Restriction enzymes, T4 ligase, a gel purification kit, and a plasmid miniprep kit were purchased from Thermo Scientific (Waltham, Massachusetts, U.S.A.). All primers were synthesized by Integrated DNA Technologies (Coralville, IA, U.S.A.). All reagents were purchased from Sigma Aldrich (St. Louis, MO, U.S.A.). *E. coli* DH10B was used for cloning purposes, and *E. coli* BL21 (DE3) was used for fluorescence characterization and fatty acid production.

**Plasmids and Strains.** Plasmid pBFR1k-RFP was constructed from phage  $P_{A1}$  promoter by placing two FapRO sites flanking the –10 region of the promoter using a one-step Golden-Gate DNA assembly method.<sup>45</sup> *Acc* overexpression plasmid pE7a-*acc* was constructed by cloning *accDA* and *accBC* from the *E. coli* genome 3' of two separate T7 promoters. Gene *fapR* was amplified from *B. subtilis* genomic DNA and cloned 3' of the  $P_{BAD}$  promoter in a BioBrick plasmid pBbA8c-RFP,<sup>46</sup> yielding pA8c-FapR. Plasmids pE7a-0 and pA8c-0 were constructed from pE7a-*acc* and pA8c-FapR by restriction digestion using *Bam*HI/*Bgl*II to remove the corresponding genes. The empty vectors were later purified and ligated. To create fatty acid-producing strain, a cytosolic thioesterase gene

*tesA* (*'tesA*; leader sequence deleted) was cloned under the control of  $P_{Tet}$ , giving pA2c-*tesA*. To create pBFR1k-RFP-8FapR, the  $P_{BAD}$ -FapR operon in pA8c-FapR was amplified and inserted to pBFR1k-RFP at 5' of the  $P_{FR1}$ -RFP operon using the Golden-Gate assembly method. To create pBFR1k-lacI-8FapR, *lacI* was first amplified from the *E. coli* genome to construct plasmid pBFR1k-lacI. The  $P_{BAD}$ -FapR operon from pA8c-FapR was then amplified and inserted to pBFR1k-lacI at 5' of the  $P_{FR1}$ -lacI operon. Plasmids pBFR1k-RFP-8MFapR and pBFR1k-lacI-8MFapR were constructed by site-directed mutagenesis (R106A and G107V) of pBFR1k-RFP-8FapR and pBFR1k-lacI-8FapR. Strains were created by transforming the corresponding plasmids into BL21 (DE3) competent cells (Table 2) by electroporation.

**Cell Growth and Fluorescence Assay.** Cell growth curves and cell culture fluorescence were recorded on an Infinite F200PRO (TECAN) plate reader. Strains were first cultivated overnight in Luria–Bertani (LB) medium (220 rpm, 37 °C) supplemented with appropriate antibiotics (50 mg/L ampicillin, 50 mg/L kanamycin, and 30 mg/L chloramphenicol). The overnight LB cultures were inoculated 2% v/v into fresh LB medium. Cells were induced at OD<sub>600</sub> of 0.6 with varied IPTG concentrations (0, 1, 4, 10, 40, 100, 400, 1000 μM). Cells were incubated in a 96-well plate inside the plate reader with shaking (218.3 rpm, 37 °C). Relative cell density (in arbitrary units) was measured by monitoring absorption at 600 nm, and fluorescence was recorded using an excitation wavelength of  $535 \pm 9$  nm and an emission wavelength of  $620 \pm 20$  nm. Data were taken every 1000 s until cell culture reached stationary phase. Fluorescence from the wild-type *E. coli* BL21 (DE3) cell culture was used as background, and was subtracted from all fluorescence measurements. The background-corrected fluorescence was later normalized by OD<sub>600</sub> and reported. The results were fitted using the Hill equation (Figure 2b, Figure 3a and d).

For measurement in minimal medium, the LB overnight culture was used to inoculate minimal medium (M9 medium supplemented with 75 mM MOPS, 2 mM MgSO<sub>4</sub>, 1 mg/L thiamine, 10 μM FeSO<sub>4</sub>, 0.1 mM CaCl<sub>2</sub> and micronutrients including 3 μM (NH<sub>4</sub>)<sub>6</sub>Mo<sub>7</sub>O<sub>24</sub>, 0.4 mM boric acid, 30 μM CoCl<sub>2</sub>, 15 μM CuSO<sub>4</sub>, 80 μM MnCl<sub>2</sub>, and 10 μM ZnSO<sub>4</sub>) with 2% glucose and appropriate antibiotics and incubated at 37 °C for overnight. The overnight culture in minimal medium was then used to inoculate a fresh minimal medium with an initial OD of 0.08, and grown to an OD<sub>600</sub> of 0.6 for induction. Cells were induced with varied amounts of arabinose (0%, 0.0001%, 0.001%, 0.01%, 0.1%) and IPTG (0, 4, 10, 40, 100, 400, 1000 μM) and incubated in a 96-well plate inside the plate reader. Data were recorded using the same method as described above.

**Malonyl-CoA Quantification.** To quantify cellular malonyl-CoA levels, overnight culture of strain SAcc1 was used to inoculate 5 mL of fresh minimal medium with 2% glucose and appropriate antibiotics for adaptation. The overnight culture was then inoculated into minimal medium with an initial OD<sub>600</sub> of 0.08. The cultures were induced with 0, 10, 40, 100, 400, 1000 μM of IPTG when OD<sub>600</sub> reached 0.6. After 10 h, 2 mL cultures were rapidly collected and centrifuged at 14,000 rpm for 30 s at 4 °C. The supernatant was immediately removed. The pellets were flash frozen using liquid nitrogen and stored at –80 °C until LC–MS analysis. To quantify malonyl-CoA concentrations, each sample was extracted with 100 μL of a solution containing 90% acetonitrile (ACN), 10% formic acid with 1 μM <sup>13</sup>C<sub>3</sub> malonyl-CoA and zirconia beads by vortexing

for 3 min. The insoluble material was removed by centrifugation; then the supernatant was filtered before LC–MS. Eight microliters were injected on a 2.1 mm × 50 mm Onyx C18 column (Phenomenex). The metabolites were separated using a linear gradient from 100% A (10 mM NH<sub>4</sub>HCO<sub>3</sub>) to 75% B (90% ACN 10 mM NH<sub>4</sub>HCO<sub>3</sub>) over 14 min followed by re-equilibration at initial conditions for 6 min using a 1200 LC system (Agilent). Mass spectra were recorded using a wide SIM scan (*m/z* 845–865) in a negative profile mode at a resolution of 60,000 on an LTQ-Velos Pro Orbitrap (Thermo-Fisher Scientific). Data were analyzed manually using the QualBrowser application of Xcalibur (Thermo-Fisher Scientific). Chromatograms were extracted for both the natural abundance malonyl-CoA and the <sup>13</sup>C<sub>3</sub> malonyl-CoA. The amount of natural abundance malonyl-CoA was determined by calculating the ratio of the peak area of the natural abundance peak to the peak area of the <sup>13</sup>C<sub>3</sub> peak.

**Fatty Acid Production Analysis.** The FA1, FA2, and FA3 strains were inoculated into LB medium with appropriate antibiotics. The overnight culture was inoculated 2% v/v into minimal medium containing appropriate antibiotics for adaptation. The overnight cultures in minimal medium were used to inoculate 25 mL of fresh minimal medium with an initial OD<sub>600</sub> of 0.08. Cells were induced when OD<sub>600</sub> reached 0.6. The large culture volume ensured that a lot of culture remained at the end, thus avoiding inaccuracies caused by evaporation and different oxygen-transfer rates. All strains were induced with 200 nM of aTc for thioesterase expression. Strains FA2 and FA3 were induced with 0.01% arabinose and 0.1 mM IPTG. Samples at several time points were collected, and cell growth was monitored using the above-mentioned method. The collected samples were stored at –80 °C until fatty acid quantification.

**Fatty Acid Quantification.** Fatty acid titers were quantified using a previously published method.<sup>23</sup> Specifically, 0.5 mL of cell culture was acidified with 50 μL of concentrated HCl (12N). The fatty acids were extracted twice with 0.5 mL ethyl acetate, which was spiked with 50 μg/mL of C<sub>19:0</sub> fatty acid methyl ester as an internal standard. The extracted fatty acids were derivatized to fatty acid methyl esters (FAME) by adding 10 μL concentrated HCl, 90 μL methanol and 100 μL of TMS-diazomethane, and incubated at room temperature for 15 min. FAME was then analyzed by a GC–MS (Hewlett-Packard model 7890A, Agilent Technologies) equipped with a DB5-MS column (J&W Scientific) and a mass spectrometer (5975C, Agilent Technologies). For each sample, the column was equilibrated at 80 °C for 1 min, followed by a ramp to 280 °C at 30 °C/min, and was then held at this temperature for 3 min. Final FAME concentration was analyzed on the basis of the FAME standard curve obtained from standard FAME mix (GLC-20 and GLC-30, Sigma Aldrich).

## ■ ASSOCIATED CONTENT

### 📄 Supporting Information

This material is available free of charge via the Internet at <http://pubs.acs.org>.

## ■ AUTHOR INFORMATION

### Corresponding Author

\*E-mail: [fzhang@seas.wustl.edu](mailto:fzhang@seas.wustl.edu)

### Notes

The authors declare no competing financial interest.

## ■ ACKNOWLEDGMENTS

This work was supported by Washington University in St. Louis, the International Center for Advanced Renewable Energy and Sustainability (I-CARES), and the Defense Advanced Research Projects Agency (D13AP00038). The authors thank Keasling lab for providing the Biobrick plasmids, the *E. coli* thioesterase, and the *S. cerevisiae* acetyl-CoA carboxylase genes.

## ■ REFERENCES

- (1) Peralta-Yahya, P. P., Zhang, F., del Cardayre, S. B., and Keasling, J. D. (2012) Microbial engineering for the production of advanced biofuels. *Nature* 488, 320–328.
- (2) Gronenberg, L. S., Marcheschi, R. J., and Liao, J. C. (2013) Next generation biofuel engineering in prokaryotes. *Curr. Opin. Chem. Biol.* 17, 462–471.
- (3) Curran, K. A., and Alper, H. S. (2012) Expanding the chemical palate of cells by combining systems biology and metabolic engineering. *Metab. Eng.* 14, 289–297.
- (4) Ajikumar, P. K., Xiao, W. H., Tyo, K. E., Wang, Y., Simeon, F., Leonard, E., Mucha, O., Phon, T. H., Pfeifer, B., and Stephanopoulos, G. (2010) Isoprenoid pathway optimization for Taxol precursor overproduction in *Escherichia coli*. *Science* 330, 70–74.
- (5) Ro, D. K., Paradise, E. M., Ouellet, M., Fisher, K. J., Newman, K. L., Ndungu, J. M., Ho, K. A., Eachus, R. A., Ham, T. S., Kirby, J., Chang, M. C., Withers, S. T., Shiba, Y., Sarpong, R., and Keasling, J. D. (2006) Production of the antimalarial drug precursor artemisinin acid in engineered yeast. *Nature* 440, 940–943.
- (6) Xue, Z., Sharpe, P. L., Hong, S. P., Yadav, N. S., Xie, D., Short, D. R., Damude, H. G., Rupert, R. A., Seip, J. E., Wang, J., Pollak, D. W., Bostick, M. W., Bosak, M. D., Macool, D. J., Hollerbach, D. H., Zhang, H., Arcilla, D. M., Bledsoe, S. A., Croker, K., McCord, E. F., Tyreus, B. D., Jackson, E. N., and Zhu, Q. (2013) Production of omega-3 eicosapentaenoic acid by metabolic engineering of *Yarrowia lipolytica*. *Nat. Biotechnol.* 31, 734–740.
- (7) Agnew, D. E., Stevermer, A. K., Youngquist, J. T., and Pflieger, B. F. (2012) Engineering *Escherichia coli* for production of C(1)(2)-C(1)(4) polyhydroxyalkanoate from glucose. *Metab. Eng.* 14, 705–713.
- (8) Martin, V. J., Pitera, D. J., Withers, S. T., Newman, J. D., and Keasling, J. D. (2003) Engineering a mevalonate pathway in *Escherichia coli* for production of terpenoids. *Nat. Biotechnol.* 21, 796–802.
- (9) Keasling, J. D. (2010) Manufacturing molecules through metabolic engineering. *Science* 330, 1355–1358.
- (10) Zhang, F., Ouellet, M., Bath, T. S., Adams, P. D., Petzold, C. J., Mukhopadhyay, A., and Keasling, J. D. (2012) Enhancing fatty acid production by the expression of the regulatory transcription factor FadR. *Metab. Eng.* 14, 653–660.
- (11) Woodruff, L. B., Boyle, N. R., and Gill, R. T. (2013) Engineering improved ethanol production in *Escherichia coli* with a genome-wide approach. *Metab. Eng.* 17, 1–11.
- (12) Kurland, C. G., and Dong, H. (1996) Bacterial growth inhibition by overproduction of protein. *Molecular Microbiology* 21, 1–4.
- (13) Tyo, K. E., Ajikumar, P. K., and Stephanopoulos, G. (2009) Stabilized gene duplication enables long-term selection-free heterologous pathway expression. *Nat. Biotechnol.* 27, 760–765.
- (14) De Mey, M., Maertens, J., Lequeux, G. J., Soetaert, W. K., and Vandamme, E. J. (2007) Construction and model-based analysis of a promoter library for *E. coli*: An indispensable tool for metabolic engineering. *BMC Biotechnol.*, DOI: 10.1186/1472-6750-7-34.
- (15) Alper, H., Fischer, C., Nevoigt, E., and Stephanopoulos, G. (2005) Tuning genetic control through promoter engineering. *Proc. Natl. Acad. Sci. U.S.A.* 102, 12678–12683.
- (16) Salis, H. M., Mirsky, E. A., and Voigt, C. A. (2009) Automated design of synthetic ribosome binding sites to control protein expression. *Nat. Biotechnol.* 27, 946.



- (17) Chubukov, V., Zuleta, I. A., and Li, H. (2012) Regulatory architecture determines optimal regulation of gene expression in metabolic pathways. *Proc. Natl. Acad. Sci. U.S.A.* 109, 5127–5132.
- (18) Kohlhaw, G. B. (2003) Leucine biosynthesis in fungi: Entering metabolism through the back door. *Microbiol. Mol. Biol. Res.* 67, 1.
- (19) Shen-Orr, S. S., Milo, R., Mangan, S., and Alon, U. (2002) Network motifs in the transcriptional regulation network of *Escherichia coli*. *Nat. Genet.* 31, 64–68.
- (20) Chin, C. S., Chubukov, V., Jolly, E. R., DeRisi, J., and Li, H. (2008) Dynamics and design principles of a basic regulatory architecture controlling metabolic pathways. *PLoS Biol.* 6, 1343–1356.
- (21) Davis, M. S., and Cronan, J. E., Jr. (2001) Inhibition of *Escherichia coli* acetyl coenzyme A carboxylase by acyl-acyl carrier protein. *J. Bacteriol.* 183, 1499–1503.
- (22) Holtz, W. J., and Keasling, J. D. (2010) Engineering static and dynamic control of synthetic pathways. *Cell* 140, 19–23.
- (23) Zhang, F. Z., Carothers, J. M., and Keasling, J. D. (2012) Design of a dynamic sensor-regulator system for production of chemicals and fuels derived from fatty acids. *Nat. Biotechnol.* 30, 354.
- (24) Zhang, F., and Keasling, J. (2011) Biosensors and their applications in microbial metabolic engineering. *Trends Microbiol.* 19, 323–329.
- (25) Farmer, W. R., and Liao, J. C. (2000) Improving lycopene production in *Escherichia coli* by engineering metabolic control. *Nat. Biotechnol.* 18, 533–537.
- (26) Anesiadis, N., Cluett, W. R., and Mahadevan, R. (2008) Dynamic metabolic engineering for increasing bioprocess productivity. *Metab. Eng.* 10, 255–266.
- (27) Gadkar, K. G., Doyle, F. J., Edwards, J. S., and Mahadevan, R. (2005) Estimating optimal profiles of genetic alterations using constraint-based models. *Biotechnol. Bioeng.* 89, 243–251.
- (28) Oyarzun, D. A., and Stan, G. B. (2012) Synthetic gene circuits for metabolic control: design trade-offs and constraints. *J. R. Soc. Interface*, DOI: 10.1098/rsif.2012.0671.
- (29) Fowler, Z. L., Gikandi, W. W., and Koffas, M. A. (2009) Increased malonyl coenzyme A biosynthesis by tuning the *Escherichia coli* metabolic network and its application to flavanone production. *Appl. Environ. Microbiol.* 75, 5831–5839.
- (30) Xu, P., Ranganathan, S., Fowler, Z. L., Maranas, C. D., and Koffas, M. A. (2011) Genome-scale metabolic network modeling results in minimal interventions that cooperatively force carbon flux towards malonyl-CoA. *Metab. Eng.* 13, 578–587.
- (31) Lennen, R. M., and Pfeleger, B. F. (2013) Microbial production of fatty acid-derived fuels and chemicals. *Curr. Opin. Biotechnol.*, DOI: 10.1016/j.copbio.2013.02.028.
- (32) Zhang, F., Rodriguez, S., and Keasling, J. D. (2011) Metabolic engineering of microbial pathways for advanced biofuels production. *Curr. Opin. Biotechnol.* 22, 775–783.
- (33) Handke, P., Lynch, S. A., and Gill, R. T. (2011) Application and engineering of fatty acid biosynthesis in *Escherichia coli* for advanced fuels and chemicals. *Metab. Eng.* 13, 28–37.
- (34) Davis, M. S., Solbiati, J., and Cronan, J. E., Jr. (2000) Overproduction of acetyl-CoA carboxylase activity increases the rate of fatty acid biosynthesis in *Escherichia coli*. *J. Biol. Chem.* 275, 28593–28598.
- (35) Lu, X., Vora, H., and Khosla, C. (2008) Overproduction of free fatty acids in *E. coli*: implications for biodiesel production. *Metab. Eng.* 10, 333–339.
- (36) Zha, W. J., Rubin-Pitel, S. B., Shao, Z. Y., and Zhao, H. M. (2009) Improving cellular malonyl-CoA level in *Escherichia coli* via metabolic engineering. *Metab. Eng.* 11, 192–198.
- (37) Miyahisa, I., Kaneko, M., Funai, N., Kawasaki, H., Kojima, H., Ohnishi, Y., and Horinouchi, S. (2005) Efficient production of (2S)-flavanones by *Escherichia coli* containing an artificial biosynthetic gene cluster. *Appl. Microbiol. Biotechnol.* 68, 498–504.
- (38) Leonard, E., Lim, K. H., Saw, P. N., and Koffas, M. A. G. (2007) Engineering central metabolic pathways for high-level flavonoid production in *Escherichia coli*. *Appl. Environ. Microbiol.* 73, 3877–3886.
- (39) Schujman, G. E., Guerin, M., Buschiazzi, A., Schaeffer, F., Llarrull, L. I., Reh, G., Vila, A. J., Alzari, P. M., and de Mendoza, D. (2006) Structural basis of lipid biosynthesis regulation in Gram-positive bacteria. *EMBO J.* 25, 4074–4083.
- (40) Schujman, G. E., Paoletti, L., Grossman, A. D., and de Mendoza, D. (2003) FapR, a bacterial transcription factor involved in global regulation of membrane lipid biosynthesis. *Dev. Cell* 4, 663–672.
- (41) Lutz, R., and Bujard, H. (1997) Independent and tight regulation of transcriptional units in *Escherichia coli* via the LacR/O, the TetR/O and AraC/I1-I2 regulatory elements. *Nucleic Acids Res.* 25, 1203–1210.
- (42) Moon, T. S., Lou, C., Tamsir, A., Stanton, B. C., and Voigt, C. A. (2012) Genetic programs constructed from layered logic gates in single cells. *Nature* 491, 249–253.
- (43) Steen, E. J., Kang, Y. S., Bokinsky, G., Hu, Z. H., Schirmer, A., McClure, A., del Cardayre, S. B., and Keasling, J. D. (2010) Microbial production of fatty-acid-derived fuels and chemicals from plant biomass. *Nature* 463, 559.
- (44) Lennen, R. M., Braden, D. J., West, R. A., Dumesic, J. A., and Pfeleger, B. F. (2010) A process for microbial hydrocarbon synthesis: Overproduction of fatty acids in *Escherichia coli* and catalytic conversion to alkanes. *Biotechnol. Bioeng.* 106, 193–202.
- (45) Engler, C., Kandzia, R., and Marillonnet, S. (2008) A one pot, one step, precision cloning method with high throughput capability. *PLoS One*, DOI: 10.1371/journal.pone.0003647.
- (46) Lee, T. S., Krupa, R. A., Zhang, F., Hajimorad, M., Holtz, W. J., Prasad, N., Lee, S. K., and Keasling, J. D. (2011) BglBrick vectors and datasheets: A synthetic biology platform for gene expression. *J. Biol. Eng.* 5, 12.